

Obesity causes very low density lipoprotein clearance defects in low-density lipoprotein receptor-deficient mice[☆]

Kimberly R. Coenen, Marnie L. Gruen, Alyssa H. Hasty*

Department of Molecular Physiology and Biophysics, Vanderbilt University Medical Center, Nashville, TN 37232-0615, USA

Received 31 August 2006; received in revised form 20 November 2006; accepted 6 December 2006

Abstract

We have reported that obese leptin-deficient mice (ob/ob) lacking the low-density lipoprotein receptor (LDLR^{-/-}) develop severe hyperlipidemia and spontaneous atherosclerosis. In the present study, we show that obese leptin receptor-deficient mice (db/db) lacking LDLR have a similar phenotype, even in the presence of elevated plasma leptin levels. We investigated the mechanism for the hyperlipidemia in obese LDLR^{-/-} mice by comparing lipoprotein production and clearance rates in C57BL/6, ob/ob, LDLR^{-/-} and ob/ob;LDLR^{-/-} mice. Hepatic triglyceride production rates were equally increased (~1.4-fold, $P < .05$) in both LDLR^{-/-} and ob/ob;LDLR^{-/-} mice compared to C57BL/6 and ob/ob mice. LDL clearance was decreased (~1.3-fold, $P < .01$) to a similar extent in LDLR^{-/-} and ob/ob;LDLR^{-/-} mice compared to C57BL/6 and ob/ob controls. While VLDL clearance was delayed in LDLR^{-/-} compared to C57BL/6 and ob/ob mice (2-fold, $P < .001$), this delay was exaggerated in ob/ob;LDLR^{-/-} mice (3.8-fold, $P < .001$). The VLDL clearance defects were due to decreased hepatic uptake compared to C57BL/6 (54% and 26% for LDLR^{-/-} and ob/ob;LDLR^{-/-}, respectively, $P < .001$). When VLDL was collected from C57BL/6, ob/ob, LDLR^{-/-}, and ob/ob;LDLR^{-/-} donors and injected into LDLR^{-/-} recipient mice, counts remaining in the liver were 1.4-fold elevated in mice receiving LDLR^{-/-} VLDL and 2-fold increased in mice receiving ob/ob;LDLR^{-/-} VLDL compared to controls receiving C57BL/6 VLDL ($P < .01$). Thus, the increase in plasma lipoproteins in ob/ob;LDLR^{-/-} mice is caused by delayed VLDL clearance. This appears to be due to defects in both the liver and the lipoproteins themselves in these obese mice.

© 2007 Elsevier Inc. All rights reserved.

Keywords: Leptin; Hyperlipidemia; Lipoprotein clearance; Hepatic triglyceride production

1. Introduction

The prevalence of obesity has risen to epidemic proportions during the past two decades. This alarming trend has resulted in a host of accompanying metabolic disorders such as insulin resistance, hypertension and dyslipidemia in what is referred to as the metabolic syndrome [1]. Individuals with the metabolic syndrome are known to have an increased risk of developing diabetes and cardiovascular disease [2,3]. The dyslipidemia that develops in obese humans is often characterized by elevated VLDL triglycerides (TGs) and the presence of small dense LDL particles [4,5] in a pro-atherogenic lipoprotein profile [6]. Although the association

between obesity and dyslipidemia is well established, the mechanism by which obesity precipitates elevations in plasma TGs is not completely understood.

Leptin and leptin receptor-deficient mice (ob/ob and db/db, respectively) were originally derived from separate spontaneous mutations [7]. These, and other mouse models of obesity, have been analyzed for both dyslipidemia and atherosclerotic lesion development, with the expectation that both would be aggravated by the obesity [8,9]. Plasma TC levels in the ob/ob and db/db mice are elevated; however, this is due to an increase in atheroprotective high-density lipoproteins (HDL) [10,11]. These obese mice are therefore resistant to atherosclerotic lesion formation, even when placed on a high-fat diet [9]. We [12,13], and others [14–16], have previously crossed the ob/ob mice onto a background of low-density lipoprotein receptor (LDLR) deficiency. The ob/ob;LDLR^{-/-} mice develop severe hyperlipidemia characterized by dramatic elevations in both TC and TG levels even when maintained on a chow diet.

[☆] Notice of support: This work was supported by the American Heart Association (0330011N), the Diabetes Research and Training Center (DK20593) and the Clinical Nutrition Research Unit (DK26657). AH Hasty is also supported by the American Diabetes Association (1-04-JF-20).

* Corresponding author. Fax: +1 615 322 8973.

E-mail address: alyssa.hasty@vanderbilt.edu (A.H. Hasty).

Thus, these mice are useful not only in obesity-related atherosclerosis studies, but also as a model to determine mechanisms by which obesity potentiates lipoprotein metabolism defects.

The processing and clearance of VLDL require the coordinated function of multiple apoproteins, lipolytic enzymes and lipoprotein receptors. During their synthesis, and while in circulation, VLDL acquires exchangeable apoproteins E and C. ApoC1 and apoC3 inhibit lipolysis, while apoC2 is an activator of lipoprotein lipase (LPL), promoting the lipolysis of TG from VLDL. VLDL remnants pass through fenestrations in the hepatic endothelial cell layer and can be further lipolyzed by hepatic lipase (HL) in the space of Disse. VLDL remnants are cleared from the liver through several different receptor-mediated mechanisms. LDLRs clear LDL and VLDL through binding of apoB100 and apoE, respectively. Heparan sulfate proteoglycans (HSPGs) can assist in the clearance of lipoproteins directly, or by facilitating LDLR-related protein (LRP)-mediated clearance. In the current study, we investigated these various stages of VLDL metabolism to determine the mechanisms by which obesity potentiates hyperlipidemia in ob/ob;LDLR^{-/-} mice.

2. Materials and methods

2.1. Mice

All mice used in these studies were on a C57BL/6 background. They were originally purchased from Jackson Laboratories (Bar Harbor, ME, USA) and were propagated within the animal care facility at Vanderbilt University. Both ob/ob;LDLR^{-/-} and db/db;LDLR^{-/-} mice were produced by intercrossing ob/+ and db/+ with LDLR^{-/-} mice. Mice were given free access to chow diet and water, and were fasted for 5–6 h before all blood collections. Mice were bled from the retro-orbital venous plexus using heparinized capillary collection tubes. Blood was placed in tubes containing EDTA and placed on ice. Plasma was separated by centrifugation and stored in aliquots at -80°C until TC, TGs and nonesterified fatty acid (NEFA) analyses could be completed. All animal care and experimental procedures were performed according to the regulations of the Institutional Animal Care and Usage Committee of Vanderbilt University.

2.2. Measurement of plasma metabolic parameters

TC and TG levels were measured using enzymatic kits from Raichem (San Diego, CA, USA) according to the manufacturer's instructions. Plasma NEFA measurements were conducted using the NEFA C kit by Wako (Neuss, Germany). Fast performance liquid chromatography (FPLC) assays were performed by separating 100 µl of plasma on a Superose 6 column (Amersham Biosciences, Sweden) at a flow rate of 0.5 ml/min. Forty fractions of 0.5 ml were collected and cholesterol levels were measured in fractions

11–40. VLDL particles elute in fractions 15–18, LDL in fractions 19–25 and HDL in fractions 26–34. The previously reported LDL/HDL1 in ob/ob mice [10] has a size distribution between that of LDL and HDL and appears in fractions 24–28.

2.3. Separation of VLDL, LDL and HDL by ultracentrifugation

Plasma samples were collected from five mice in each group after a 5-h fast. Plasma (100 µl) from each mouse was separated into VLDL ($d < 1.019$ g/L), LDL ($d = 1.019$ – 1.040 g/L) and HDL ($d = 1.040$ – 1.210 g/L) by ultracentrifugation on a Beckman TLX ultracentrifuge. Lipoprotein fractions were dialyzed and concentrated by repeated centrifugation over microcon columns (Millipore Corp., Bedford, MA, USA). All samples were brought back to a 100-µl volume followed by measurement of TC as described above.

2.4. Lipoprotein production studies

Mice were fasted overnight and then bled via the retro-orbital venous plexus for baseline analysis. The mice were then injected with tyloxapol (purchased from Sigma and hereafter referred to as Triton) at a concentration of 500 mg/kg body weight. Subsequent blood collection occurred at 1 and 2 h after Triton injection and plasma were isolated for TG analysis. Lipoprotein production rates were linear for all mice through the 2-h time course. The slope of the line from baseline to 2 h was used to calculate TG production rate.

2.5. Plasma volume measurements

Alexafluor 568-labeled bovine serum albumin (BSA) (Invitrogen, Carlsbad, CA, USA) was injected into mice via the tail vein at a concentration of 50 mg/ml. At 5 min postinjection, mice were bled, and the plasma separated. Both the originally injected BSA and plasma were serially diluted, and the fluorescence emission measured on a Polarstar Galaxy plate reader by BMG Laboratories. Data analysis was performed using Fluorstar Galaxy software 4.11-0. Plasma concentrations of AlexBSA were determined based upon the fluorescence and were used to calculate the plasma volume as a percentage of body weight. Plasma volume was calculated at $3.2 \pm 0.57\%$ of body weight for lean mice and $1.8 \pm 0.25\%$ of body weight for obese mice ($n = 10$ – 12 per group). These calculations were therefore used for lipoprotein clearance studies (Experiments 1 and 2) described below.

2.6. Lipoprotein clearance studies

Experiment 1: Plasma was collected from LDLR^{-/-} mice and Triton-treated C57BL/6 mice for preparation of LDL ($d = 1.019$ – 1.04 g/L) and VLDL ($d < 1.019$ g/L), respectively, by serial ultracentrifugation in a Beckman TLX ultracentrifuge (Fig. 3). The lipoproteins were labeled with ¹²⁵I•NaI (Amersham Biosciences, Sweden) using the MacFarlane method as described [17–19]. Labeled

lipoproteins had a specific activity between 200 and 250 CPM/ng. Recipient C57BL/6, LDLR^{-/-}, ob/ob and ob/ob;LDLR^{-/-} mice were injected with 5 µg of protein via the tail vein. At 10 min, 1 h, 4 h and 18 h postinjection, blood was collected from the retro-orbital plexus, and plasma was isolated to determine the percent of injected counts remaining (assuming a plasma volume based upon body weight as described above).

Experiment 2: VLDL ($d < 1.019$ g/L) was prepared from ob/ob;LDLR^{-/-} mice by ultracentrifugation. C57BL/6, LDLR^{-/-}, ob/ob and ob/ob;LDLR^{-/-} mice were sacrificed 5 min following ¹²⁵I-VLDL injection, perfused, and livers were excised (Fig. 4). A portion of the liver was analyzed for radioactive counts which were then normalized to total liver weight. Plasma and liver counts are presented as percentage of injected counts.

Experiment 3: Plasma was collected from C57BL/6, ob/ob, LDLR^{-/-} and ob/ob;LDLR^{-/-} mice (Fig. 6). Pooled plasma samples from each group were used to prepare $d < 1.109$ g/ml lipoproteins. These lipoproteins were labeled with ¹²⁵I and used in turnover studies in LDLR^{-/-} recipient mice. Five-minutes postinjection mice were bled, sacrificed, perfused, and livers collected for quantification of radioactivity remaining in plasma and liver as described for Experiment 2.

2.7. Hepatic lipase activity

The Hepatic Lipase Continuous Fluorometric Lipase Test from Progen (Heidelberg, Germany) was used for analysis of plasma HL activity. This assay utilizes a formulated TG substrate in which pyrene fluorescence is intramolecularly quenched in the absence of lipase. The special buffer conditions allow the selective determination of HL. In the presence of HL, the quencher is hydrolyzed and the pyrene fluorescence can be measured. The assay was adapted for use in a 96-well plate by using 2 µl of a 1:5 dilution of plasma from fasted, non-heparin-treated mice. Fluorescence intensity was read at 342 nm Ex and 400 nm Em in 1-min

intervals over a 10-min period at 37°C using a Polarstar Galaxy plate reader. The slopes of the samples were compared to the slope of a standard (unquenched fluorescent derivative of the substrate) ranging from 1.4 to 22.5 pmol/ml.

2.8. Real-time RT-PCR analyses

Upon sacrifice, 6-month-old fasted mice ($n = 6-10$ for each group) were perfused and livers were collected and immediately snap frozen. Total RNA was isolated using Trizol reagent according to the manufacturer's instructions (Invitrogen). All primer/probe sets used for real-time RT-PCR of mouse liver samples were purchased through the "Assays-on-demand" program (Applied Biosystems, Foster City, CA, USA). Real-time RT-PCR reactions for each gene were performed simultaneously for all RNA samples in 96-well plates on an ABI 7700 machine. The Ct values of each gene were normalized to 18S for individual samples. Final relative concentrations were determined according to the $\Delta\Delta$ Ct method [20]. Data are presented as expression relative to the C57BL/6 group.

2.9. Sodium dodecyl sulfate Gels

Radiolabeled VLDL samples ($d < 1.019$ g/L) isolated from C57BL/6, ob/ob, LDLR^{-/-} and ob/ob;LDLR^{-/-} mice for lipoprotein clearance in Experiment 3 were electrophoresed through 4–12% SDS gels using MES buffer (Invitrogen).

2.10. Statistical analyses

All statistical analyses were performed using ANOVA with a Bonferroni post hoc test unless otherwise indicated.

3. Results

3.1. Metabolic parameters in obese LDLR^{-/-} mice

Obesity dramatically increases plasma TC and TG levels in mice deficient in both leptin and LDLR (ob/ob;LDLR^{-/-})

Table 1
Metabolic parameters and atherosclerosis in ob/ob;LDLR^{-/-}, db/db;LDLR^{-/-} and control mice

	C57BL/6	LDLR ^{-/-}	ob/ob	db/db	ob/ob;LDLR ^{-/-}	db/db;LDLR ^{-/-}
Weight (g)	25±1	26±1	53±1 ^a	51±1 ^a	53±1 ^a	50±2 ^a
Leptin (ng/ml)	ND	ND	ND	85±13	ND	96±7
Cholesterol (mg/dl)	75±4	192±9 ^b	167±10 ^b	135±7 ^b	704±19 ^c	653±21 ^c
Triglycerides (mg/dl)	58±5	51±4	58±6	94±25	598±116 ^d	464±73 ^d
NEFA (mEq/L)	0.71±0.17	0.34±0.04	0.49±0.07	0.47±0.06	0.97±0.11 ^c	1.04±0.08 ^c
Glucose (mg/dl)	105±6	112±8	125±16	131±10	110±9	111±14
Lesion area (µm ² /section)	ND	ND	ND	ND	104,659±10,054	91,819±6185

Plasma samples from fasted 3- to 6-month-old mice were analyzed for leptin, TC, TG, NEFA and glucose levels. Atherosclerotic lesion area was measured in 8-month-old mice. Data are presented as mean±S.E.M. from 4 to 15 different mice in each group. ND indicates not determined. Statistical analyses for body weight, TC, TG, and NEFA were performed using ANOVA with Bonferroni post hoc test. Analyses for leptin (db/db vs. db/db;LDLR^{-/-}) and lesion area (ob/ob;LDLR^{-/-} and db/db;LDLR^{-/-}) were performed using an unpaired Student's *t*-test.

^a $P < .001$ compared to lean C57BL/6 and LDLR^{-/-}.

^b $P < .05$ compared to C57BL/6.

^c $P < .001$ compared to all.

^d $P < .05$ compared to all.

^e $P < .01$ compared to LDLR^{-/-}, ob/ob and db/db.

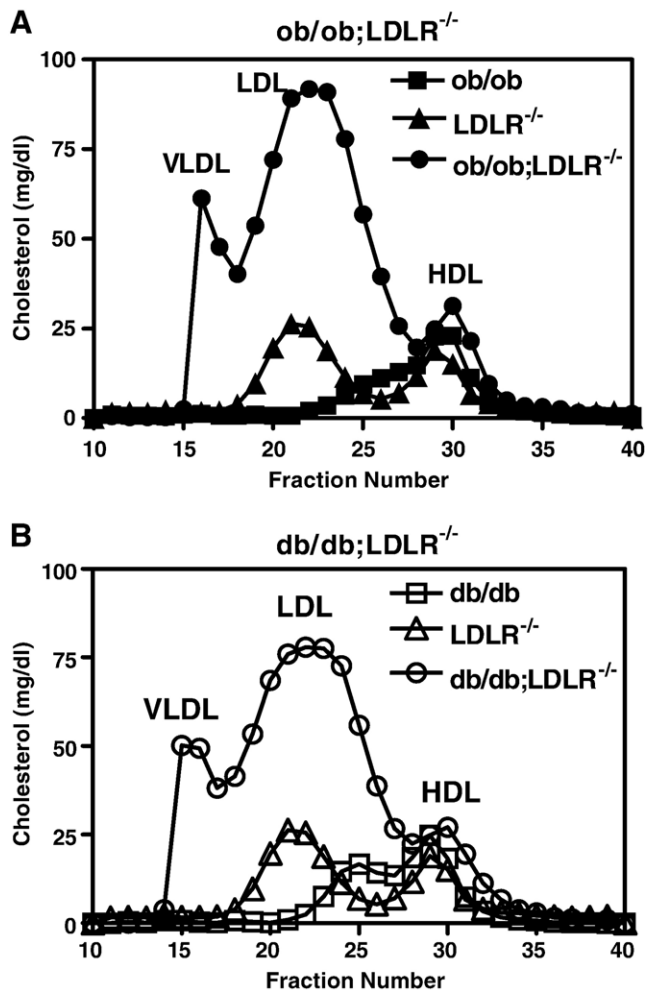


Fig. 1. Lipoprotein profiles of *ob/ob;LDLR^{-/-}* and *db/db;LDLR^{-/-}* mice. Plasma lipoproteins were separated by gel filtration chromatography and cholesterol measured in the collected fractions as described in the Materials and Methods section. (A) *ob/ob* (closed squares), *LDLR^{-/-}* (closed triangles) and *ob/ob;LDLR^{-/-}* (closed circles). (B) *db/db* (open squares), *LDLR^{-/-}* (open triangles) and *db/db;LDLR^{-/-}* (open circles). VLDL particles are in fractions 15–18, LDL in fractions 19–25 and HDL in fractions 26–34.

[12,13]. To determine whether the absence of circulating leptin contributes to hyperlipidemia in these mice, we compared *ob/ob;LDLR^{-/-}* (no plasma leptin) with leptin receptor-deficient mice also crossed onto the *LDLR^{-/-}* background (*db/db;LDLR^{-/-}*, elevated plasma leptin levels; Table 1). Both *ob/ob;LDLR^{-/-}* and *db/db;LDLR^{-/-}* mice displayed similarly elevated body weights compared to lean C57BL/6 and *LDLR^{-/-}* controls (Table 1). In addition, plasma TC, TG and NEFA levels were synergistically elevated in the *ob/ob;LDLR^{-/-}* and *db/db;LDLR^{-/-}* mice compared to *LDLR^{-/-}*, *ob/ob* and *db/db* controls (Table 1). Glucose levels were not significantly different between the six groups. Atherosclerotic lesion area was not different between the two obese *LDLR^{-/-}* groups.

Analysis of lipoprotein profiles by FPLC demonstrated similar profiles in *ob/ob;LDLR^{-/-}* and *db/db;LDLR^{-/-}*

mice with cholesterol carried primarily on VLDL and LDL (Fig. 1). These data demonstrate that the absence of circulating leptin protein itself is not responsible for the hyperlipidemia and atherosclerosis in *ob/ob;LDLR^{-/-}* mice. Because there were no differences between the *ob/ob;LDLR^{-/-}* and *db/db;LDLR^{-/-}* mice with regard to plasma lipoprotein levels, remaining studies were performed in *ob/ob;LDLR^{-/-}* mice with C57BL/6, *ob/ob* and *LDLR^{-/-}* mice used as controls.

3.2. VLDL, LDL and HDL lipid levels

Further analysis of lipoprotein cholesterol and TG content was performed using ultracentrifugation to isolate VLDL, LDL and HDL fractions. Plasma TGs were carried exclusively on VLDL (data not shown) as previously reported in experiments using FPLCs to analyze TG distribution in *ob/ob;LDLR^{-/-}* mice [13]. Confirming the FPLC results, analysis showed the absolute levels of VLDL and LDL cholesterol were elevated in *ob/ob;LDLR^{-/-}* mice. By ultracentrifugation, approximately 52% of the cholesterol was in VLDL, 24% was in the LDL fractions and 24% was present on HDL in the *ob/ob;LDLR^{-/-}* mice. This is slightly different from what appears to be a larger percent of cholesterol carried on LDL based upon FPLC analysis (Fig. 1A). It is likely that some large IDL particles that appear as LDL on FPLC actually float with VLDL at a density of $d < 1.019$ g/L during ultracentrifugation.

3.3. Hepatic TG production rates

To determine whether the elevated levels of circulating VLDL and LDL were caused by increased production of TG-rich lipoproteins, we performed Triton studies in overnight fasted mice (Fig. 2). There was a significant increase in hepatic TG production rates in the *LDLR^{-/-}* and *ob/ob;LDLR^{-/-}* mice compared to C57BL/6 and *ob/ob*

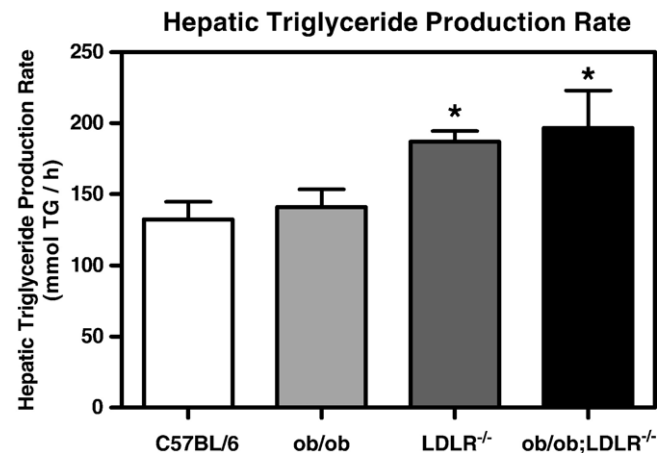


Fig. 2. Hepatic TG production rates in *ob/ob;LDLR^{-/-}* mice. C57BL/6, *ob/ob*, *LDLR^{-/-}* and *ob/ob;LDLR^{-/-}* mice were injected with Triton at a concentration of 500 mg/kg body weight. Plasma TGs were measured before, and at 1 and 2 h postinjection. TG production rates were calculated from the slope of the line created by these three points (mean \pm S.E.M., $n = 7-9$ for each group). * $P < 0.05$ compared to C57BL/6 and *ob/ob*.

controls (C57BL/6, 132 ± 12 ; ob/ob, 141 ± 13 ; LDLR^{-/-}, 187 ± 7 ; and ob/ob;LDLR^{-/-}, 197 ± 27 mmol TG/h; $P < .05$). Thus, LDLR deficiency, but not obesity, increases hepatic TG production.

3.4. Plasma and hepatic lipoprotein clearance

Evaluation of lipoprotein clearance involves an estimation of plasma volume based upon body weight. Because the increase in body weight in ob/ob and ob/ob;LDLR^{-/-} is due to increased adipose tissue, which is not as vascularized as lean body mass, we first determined the ratio of plasma volume to body weight in obese mice (described in the Materials and Methods section). Plasma volumes were determined to be 3.2% and 1.8% of body weight in lean and obese mice, respectively. This compares to a traditionally used value of 3.5% for lean mice [18,19,21]. These ratios were used to calculate plasma volume for lean and obese mice, respectively, in the lipoprotein clearance studies described below.

Radiolabeled LDL ($d = 1.019\text{--}1.040$ g/L) and VLDL ($d < 1.019$ g/L) were injected into recipient C57BL/6, ob/ob, LDLR^{-/-} and ob/ob;LDLR^{-/-} mice, and blood was collected at 10 min, 1, 4 and 18 h postinjection (Fig. 3). Similar delays in LDL clearance were detected in LDLR^{-/-} and ob/ob;LDLR^{-/-} mice compared to C57BL/6 and ob/ob mice through the 4-h time point (Fig. 3A). Likewise, VLDL clearance was delayed in LDLR^{-/-} animals (Fig. 3B), as previously reported [22]. However, the impaired VLDL clearance seen in lean LDLR^{-/-} mice was exacerbated in obese ob/ob;LDLR^{-/-} mice.

Delayed clearance of VLDL in ob/ob;LDLR^{-/-} mice was detected as early as 10 min postinjection, potentially indicating defects in the initial capture and retention of lipoproteins into the space of Disse. We therefore performed a second VLDL clearance study in which mice were sacrificed at 5 min postinjection (Fig. 4). Confirming the data shown in Fig. 3, the study showed VLDL clearance was impaired in the LDLR^{-/-} mice compared to C57BL/6 and ob/ob mice ($P < .001$) as determined from the counts remaining in plasma. In addition, the delay in VLDL clearance was amplified in ob/ob;LDLR^{-/-} mice ($P < .001$). This delay was accounted for by significantly reduced levels of VLDL taken up by livers of lean LDLR^{-/-} ($P < .05$ compared to C57BL/6 and ob/ob) and obese ob/ob;LDLR^{-/-} mice ($P < .001$ compared to all groups). Taken together, these lipoprotein clearance studies suggest that hepatic clearance of VLDL is delayed in the absence of LDLR expression, and that obesity potentiates this delay in ob/ob;LDLR^{-/-} mice.

To determine whether any genes commonly involved in remnant lipoprotein clearance were altered in the ob/ob;LDLR^{-/-} mice, we performed real-time RT-PCR analysis on liver RNA from 6-h fasted mice. Expression of the remnant lipoprotein receptor, LRP, was not different between animals. Likewise, expression of HSPG core proteins, perlecan, syndecan and glypican was not changed

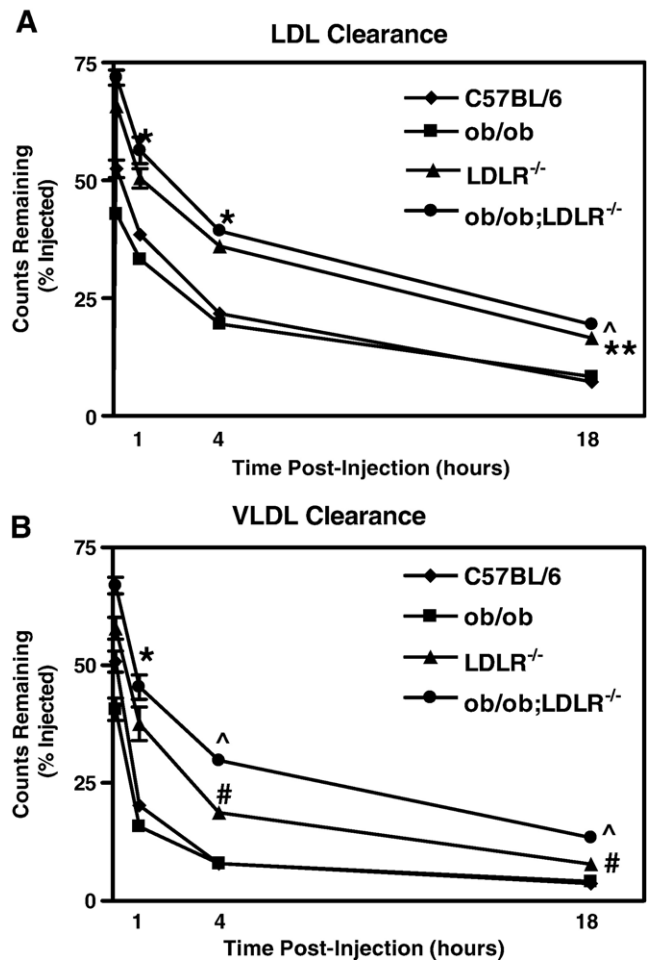


Fig. 3. LDL and VLDL clearance. LDL and VLDL were prepared by ultracentrifugation and labeled with ^{125}I as described in the Materials and Methods section. Labeled lipoproteins were injected into C57BL/6 (diamonds), ob/ob (squares), LDLR^{-/-} (triangles) and ob/ob;LDLR^{-/-} (circles) mice via the tail vein. Blood was collected from mice at 10 min, 1 h, 4 h and 18 h postinjection, and plasma isolated for radioactive count analysis. Counts remaining in the plasma are expressed as the percent injected for LDL (A) and VLDL (B). Data are presented as mean \pm S.E.M. ($n = 3$ for C57BL/6, ob/ob and LDLR^{-/-}; $n = 2$ for ob/ob;LDLR^{-/-}). * $P < .01$ compared to C57BL/6 and ob/ob; ** $P < .05$ compared to all other groups; ^ $P < .001$ compared to all other groups; # $P < .01$ compared to all other groups.

(data not shown). In addition, expression of these genes was not different between the four groups of mice in the fed state (data not shown). Thus, expression levels of LRP and proteoglycan core proteins do not appear to explain the impaired VLDL clearance.

3.5. Hepatic lipase activity

In our initial report, we provided evidence that plasma LPL activity was not different between ob/ob;LDLR^{-/-} and control mice [12]. To determine whether a reduction in HL activity could account for the delayed VLDL clearance, liver HL RNA levels and plasma activity of HL were analyzed (Fig. 5). Hepatic expression of HL was significantly reduced in ob/ob;LDLR^{-/-} compared to C57BL/6

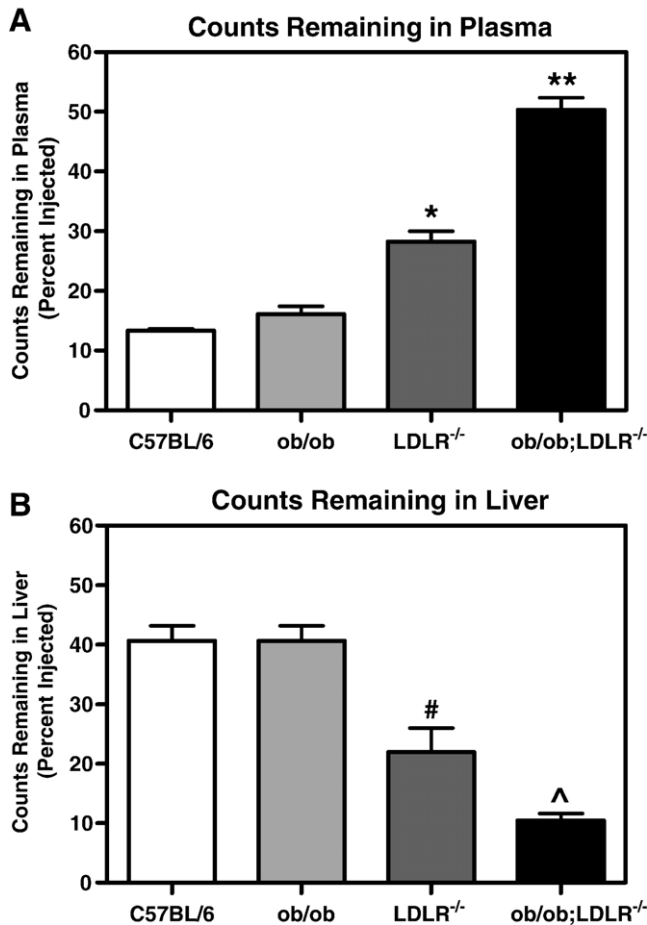


Fig. 4. VLDL Clearance — hepatic uptake. VLDL was collected from ob/ob;LDLR^{-/-} mice, labeled and injected into C57BL/6, ob/ob, LDLR^{-/-} and ob/ob;LDLR^{-/-} mice as described for Fig. 3. Mice were sacrificed 5 min following ¹²⁵I-VLDL injection, bled, perfused, and livers were excised. The counts remaining in plasma (A) and liver (B) are expressed as a percent of injected counts (mean±S.E.M., *n*=4–5 for each group). **P*<.001 compared to C57BL/6 and ob/ob; ***P*<.001 compared to all other groups; ^*P*<.05 compared to LDLR^{-/-} and *P*<.001 compared to C57BL/6 and ob/ob; #*P*<.01 compared to C57BL/6 and ob/ob.

mice (*P*<.05); however, preheparin HL activity in plasma of 6-h fasted ob/ob;LDLR^{-/-} mice was significantly increased compared to C57BL/6 and LDLR^{-/-} mice (*P*<.01). Thus, changes in circulating LPL and HL do not account for the delayed VLDL clearance seen in ob/ob;LDLR^{-/-} mice.

3.6. Ability of VLDL to act as substrate for hepatic clearance

To determine whether phenotypic differences in the VLDL itself could also contribute to delayed clearance, we isolated *d*<1.019 g/L lipoproteins from C57BL/6, ob/ob, LDLR^{-/-} and ob/ob;LDLR^{-/-} mice (Fig. 6). Apoprotein content of ¹²⁵I-labeled VLDL was assessed by SDS-PAGE (Fig. 6A). ApoE and apoB levels were increased on VLDL from ob/ob;LDLR^{-/-} mice; however, apoC levels were decreased. In contrast to its decreased presence on VLDL, hepatic apoC2 expression was significantly increased in

both ob/ob and ob/ob;LDLR^{-/-} mice compared to lean C57BL/6 and LDLR^{-/-} controls [5.3 ± 0.9 , 4.7 ± 0.5 , 1.0 ± 0.1 and 0.9 ± 0.1 (mean±S.E.M.), respectively; arbitrary units relative to C57BL/6; *P*<.001]. ApoC3 expression was increased in ob/ob livers compared to C57BL/6 (2.1 ± 0.4 vs. 1.1 ± 0.1 , respectively, *P*<.05), but was not changed in LDLR^{-/-} or ob/ob;LDLR^{-/-} mice (0.9 ± 0.1 and 1.0 ± 0.1 , respectively).

The VLDL collected from mice of the four donor genotypes was injected into LDLR^{-/-} mice to specifically analyze non-LDLR-mediated clearance. Plasma samples were collected immediately and at 5 min postinjection at which time mice were sacrificed, perfused, and livers collected. There were no differences in the amount of radiolabel remaining in plasma between the four groups of

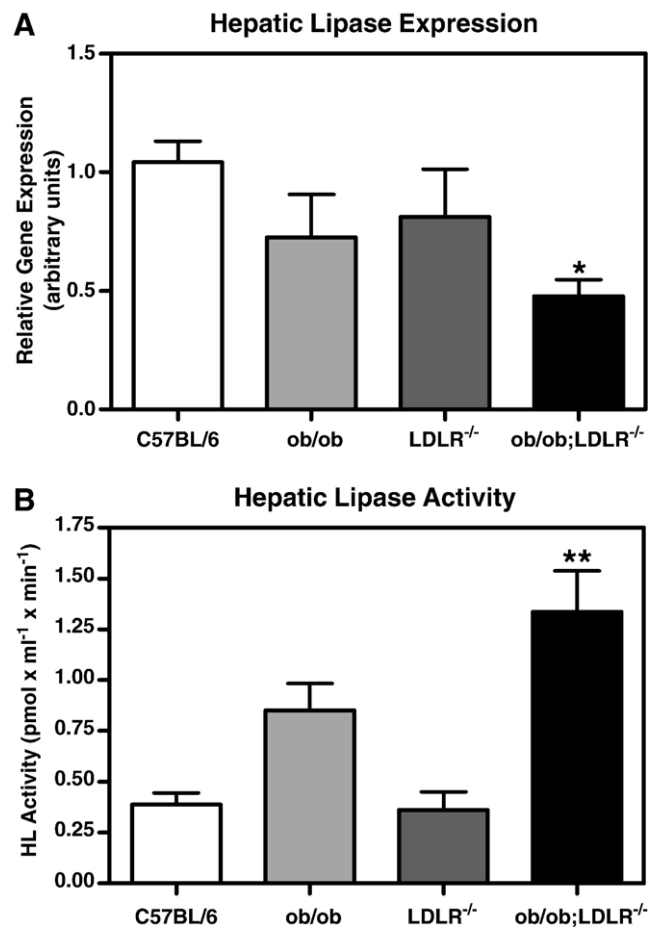
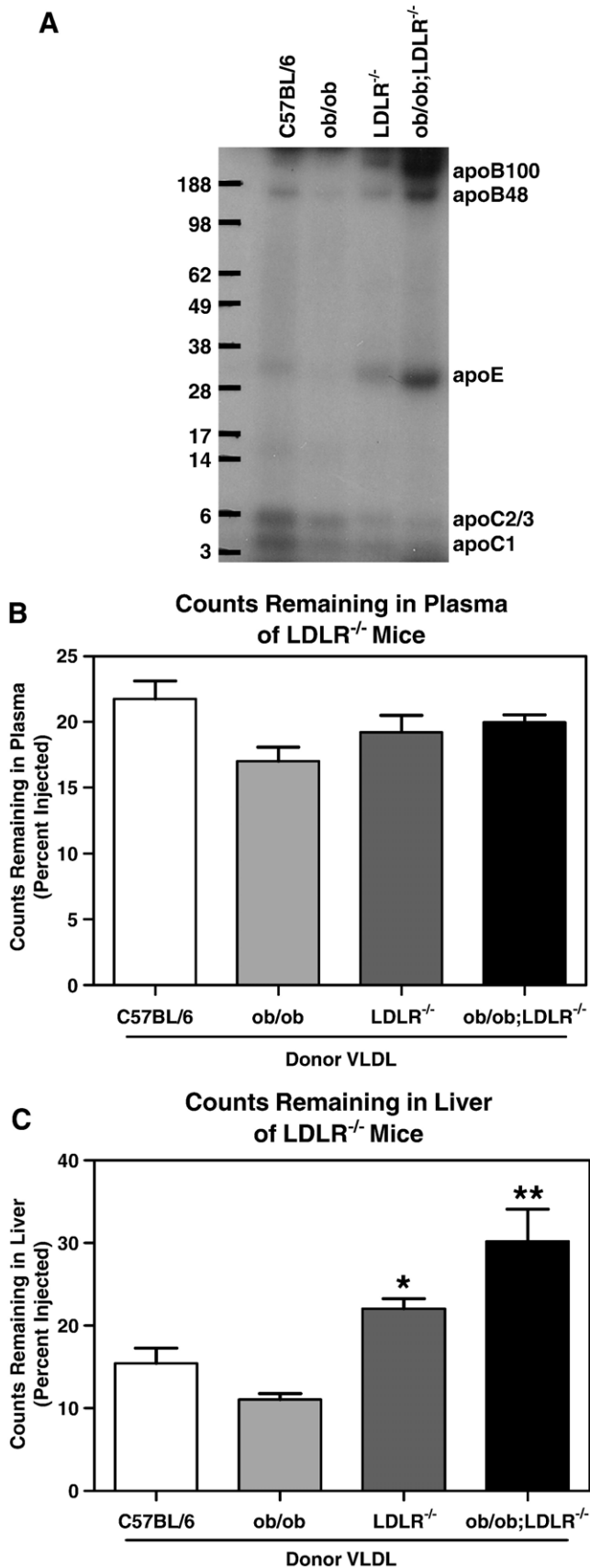


Fig. 5. Hepatic lipase gene expression and activity. C57BL/6, ob/ob, LDLR^{-/-} and ob/ob;LDLR^{-/-} mice were fasted for 6 h. Blood was collected and mice were sacrificed, perfused, and livers harvested in liquid nitrogen. (A) RNA was extracted from the liver and was used for real-time RT-PCR analysis of HL mRNA expression as described in the Materials and Methods section. (B) Hepatic lipase activity was assessed in plasma using the Hepatic Lipase Continuous Fluorometric Lipase Test (Confluolip) kit. Activity was measured at 1-min intervals over a 10-min time period at 37°C and is expressed as picomole per milliliter per minute. Data are expressed as mean±S.E.M., *n*=6–10 for each group. **P*<.05 compared to C57BL/6; ***P*<.01 compared to C57BL/6 and *P*<.001 compared to LDLR^{-/-}.



mice (Fig. 6B). Remarkably, counts remaining in livers were 1.4-fold increased in LDLR^{-/-} mice receiving VLDL from LDLR^{-/-} mice, and 2-fold higher in mice receiving VLDL from ob/ob;LDLR^{-/-} donors compared to VLDL from C57BL/6 and ob/ob mice (Fig. 6C, $P < .01$). Thus, it is possible that VLDL from ob/ob;LDLR^{-/-} mice is trapped within the hepatic sinus in the absence of LDLRs.

4. Discussion

In this study, we have analyzed the various steps of VLDL metabolism to determine the mechanism(s) responsible for severe hyperlipidemia found in obese LDLR^{-/-} mice. In our previous study, we were able to rule out dietary cholesterol intake, quantity of food intake and plasma LPL activity as contributing factors to the hyperlipidemia in ob/ob;LDLR^{-/-} mice [12]. In the current study, we analyzed hepatic TG production rates, hepatic LDL and VLDL clearance rates, HL activity, as well as hepatic expression of genes known to be involved in remnant lipoprotein clearance.

Our studies suggest two different ways in which LDLR deficiency contributes to hyperlipidemia in ob/ob;LDLR^{-/-} mice as evidenced by identical results for both LDLR^{-/-} and ob/ob;LDLR^{-/-} mice. First, hepatic TG production rates were equally increased in both groups (Fig. 2). Second, LDL clearance was equally delayed in LDLR^{-/-} and ob/ob;LDLR^{-/-} mice (Fig. 3A). Thus, increased hepatic TG production and delayed LDL clearance appear to be attributable specifically to the absence of the LDLR in this model and cannot account for the severe hyperlipidemia seen in ob/ob;LDLR^{-/-} mice.

The role of LDLR in hepatic TG production has been debated. In vitro studies in primary hepatocytes have shown that apoB100 is secreted at a 3.5-fold higher rate in LDLR^{-/-} compared to wild-type hepatocytes [23]. In contrast, in vivo studies in the LDLR-defective Watanabe heritable hyperlipidemic rabbit [24] and in LDLR^{-/-} mice [21] show no effect of LDLR deficiency on hepatic TG production. Yet, human studies have shown an increased TG production rate in familial hypercholesterolemic patients [25]. It is likely that the discrepant results from different laboratories regarding hepatic TG production in LDLR-deficient models stem from the use of different protocols. For example, in the studies in LDLR^{-/-} mice by Millar et al. [21], mice were fasted for 4 h prior to Triton injection, whereas in our studies, mice were fasted overnight.

Fig. 6. Clearance of VLDL prepared from C57BL/6, ob/ob, LDLR^{-/-} and ob/ob;LDLR^{-/-} mice in LDLR^{-/-} recipients. VLDL was prepared from C57BL/6, ob/ob, LDLR^{-/-} and ob/ob;LDLR^{-/-} mice. (A) Apoprotein content of the VLDL fractions was assessed by SDS-PAGE. (B–C) VLDL was injected into LDLR^{-/-} recipients. Mice were sacrificed after 5 min, and labeled VLDL remaining in plasma (B) and liver (C) were quantified. Data are presented as a percent of the injected counts (mean ± S.E.M., $n = 3–4$ for each group). * $P < .05$ compared to ob/ob; ** $P < .01$ compared to C57BL/6 and ob/ob.

In ob/ob;LDLR^{-/-} mice, excessive plasma lipid accumulation appears to be attributed to both the liver and the VLDL itself. First, livers of obese ob/ob;LDLR^{-/-} mice are unable to properly endocytose and clear VLDL. This is evident from our observation that while clearance of VLDL from C57BL/6 mice was delayed in lean LDLR^{-/-} mice, this defect was exaggerated in obese ob/ob;LDLR^{-/-} mice (Figs. 3B and 4). Second, VLDL collected from LDLR^{-/-} mice was trapped in livers of LDLR^{-/-} mice, an effect that was again amplified for VLDL from obese ob/ob;LDLR^{-/-} mice (Fig. 6B). Thus, it is possible that obesity influences hepatic VLDL metabolism by altering the phenotype of both the liver and circulating VLDL.

One of the primary pathways for hepatic VLDL clearance is trapping of particles by HSPGs via apoE in the space of Disse [26]. These VLDL particles can then be internalized directly or passed on to LRP for receptor-mediated uptake [27]. Unexpectedly, we found no change in expression levels of LRP, or the HSPG core proteins, syndecan, perlecan or glypican. Previous work from the Williams laboratory has shown that both syndecan and perlecan can mediate catabolism of remnant lipoproteins [28,29]. Furthermore, in a type 2 diabetic mouse model, clearance of β -VLDL was delayed due to reduced trapping in the liver caused by reduced hepatic perlecan HSPG [30]; and in a type 1 diabetic mouse model, reduced perlecan core protein and HSPG sulfation was detected [31]. While we did not detect any differences in the expression levels of HSPG core proteins, we cannot rule out that post-translational modifications, such as the composition or number of glycosaminoglycan side chains, is altered on HSPGs within the hepatic sinus of ob/ob;LDLR^{-/-} mice.

The role of apoCs (apoC1, apoC2 and apoC3) in VLDL lipolysis and clearance is complex. Both apoC1 and apoC3 play primary roles in the metabolism of remnant lipoproteins by inhibiting LPL and HL activity as well as by interfering with the clearance of these particles via apoE, LRP and HSPGs [32–36]. In contrast, apoC2 is required for the activation of LPL, and humans with apoC2 deficiency develop hypertriglyceridemia [37–39]. In fact, even reduced levels of functional apoC2 in individuals heterozygous for a mutant allele result in hypertriglyceridemia [40]. VLDL prepared from LDLR^{-/-} mice had reduced apoC content relative to apoE and apoB, a ratio that was even lower in ob/ob;LDLR^{-/-} mice (Fig. 6A). Thus, the reduced apoC2 content on VLDL from obese ob/ob;LDLR^{-/-} mice may contribute to defective VLDL metabolism leading to hyperlipidemia in these mice.

By comparing ob/ob;LDLR^{-/-} and db/db;LDLR^{-/-} mice, we provide evidence that the metabolic consequences of leptin signaling deficiency, rather than the presence or absence of circulating leptin itself, are responsible for the hyperlipidemia noted in obese LDLR^{-/-} mice. This is the first report of synergistic increases in hyperlipidemia in mice lacking both leptin receptor and LDLR (db/db;LDLR^{-/-}).

The hyperlipidemia that develops in db/db;LDLR^{-/-} is identical to that found in ob/ob;LDLR^{-/-} mice. Additionally, these animals develop spontaneous atherosclerosis. This model will be useful in future studies to determine the role of hyperleptinemia in obesity-related atherosclerosis.

Our data suggest that obesity contributes to VLDL clearance defects, rather than lipoprotein production or LDL clearance in the ob/ob;LDLR^{-/-} mouse model. However, further studies are needed to determine whether changes in HSPG sulfation in the liver and/or reduced apoC2 on VLDL are responsible for the hyperlipidemia seen in ob/ob;LDLR^{-/-} mice. In conclusion, our studies highlight the impact of not only the liver, but also the VLDL itself, on the development of obesity-related hyperlipidemia.

References

- [1] Ford ES, Giles WH, Dietz WH. Prevalence of the metabolic syndrome among US adults: findings from the third national health and nutrition examination survey. *J Am Med Assoc* 2002;287:356–9.
- [2] Reilly MP, Rader DJ. The metabolic syndrome: more than the sum of its parts? *Circulation* 2003;108:1546–51.
- [3] Isomaa B, Almgren P, Tuomi T, Forsen B, Lahti K, Nissen M, et al. Cardiovascular morbidity and mortality associated with the metabolic syndrome. *Diabetes Care* 2001;24:683–9.
- [4] Denke MA. Connections between obesity and dyslipidaemia. *Curr Opin Lipidol* 2001;12:625–8.
- [5] Executive Summary of The Third Report of The National Cholesterol Education Program (NCEP) Expert Panel on Detection, Evaluation, and Treatment of High Blood Cholesterol in Adults (Adult Treatment Panel III). *J Am Med Assoc* 2001;285:2486–97.
- [6] Fruchart JC, Nierman MC, Stroes ES, Kastelein JJ, Duriez P. New risk factors for atherosclerosis and patient risk assessment. *Circulation* 2004;109:III15–III19.
- [7] Ingalls AM, Dickie MM, Snell GD. Obese, a new mutation in the house mouse. *J Hered* 1950;41:317–8.
- [8] Nishina PM, Lowe S, Wang J, Paigen B. Characterization of plasma lipids in genetically obese mice: the mutants obese, diabetes, fat, tubby, and lethal yellow. *Metabolism* 1994;43:549–53.
- [9] Nishina PM, Naggert JK, Verstuyft J, Paigen B. Atherosclerosis in genetically obese mice: the mutants obese, diabetes, fat, tubby, and lethal yellow. *Metabolism* 1994;43:554–8.
- [10] Silver DL, Jiang X-C, Tall AR. Increased high density lipoprotein (HDL), defective hepatic catabolism of apoA-I and apoA-II, and decreased apoA-I mRNA in ob/ob mice. *J Biol Chem* 1999;274:4140–6.
- [11] Silver DL, Wang N, Tall AR. Defective HDL particle uptake in ob/ob hepatocytes causes decreased recycling, degradation, and selective lipid uptake. *J Clin Invest* 2000;105:151–9.
- [12] Hasty A, Shimano H, Osuga J, Namatame I, Takahashi A, Yahagi N, et al. Severe hypercholesterolemia, hypertriglyceridemia, and atherosclerosis in mice lacking both leptin and the low density lipoprotein receptor. *J Biol Chem* 2001;276:37402–8.
- [13] Gruen ML, Saraswathi V, Nuotio-Antar AM, Plummer MR, Coenen KR, Hasty AH. Plasma insulin levels predict atherosclerotic lesion burden in obese hyperlipidemic mice. *Atherosclerosis* 2006;186:54–64.
- [14] Mertens A, Verhamme P, Bielicki JK, Phillips MC, Quarck R, Verreth W, et al. Increased low-density lipoprotein oxidation and impaired high-density lipoprotein antioxidant defense are associated with increased macrophage homing and atherosclerosis in dyslipidemic obese mice: LCAT gene transfer decreases atherosclerosis. *Circulation* 2003;107:1640–6.

- [15] Verreth W, De Keyzer D, Pelat M, Verhamme P, Ganame J, Bielicki JK, et al. Weight-loss-associated induction of peroxisome proliferator-activated receptor- α and peroxisome proliferator-activated receptor- γ correlate with reduced atherosclerosis and improved cardiovascular function in obese insulin-resistant mice. *Circulation* 2004;110:3259–69.
- [16] Verreth W, Ganame J, Mertens A, Bernar H, Herregods MC, Holvoet P. Peroxisome proliferator-activated receptor- α , γ -agonist improves insulin sensitivity and prevents loss of left ventricular function in obese dyslipidemic mice. *Arterioscler Thromb Vasc Biol* 2006;26:922–8.
- [17] McFarlane AS. Efficient trace-labeling of proteins with iodine. *Nature* 1958;132:53.
- [18] Fazio S, Hasty AH, Carter KJ, Murray AB, Price JO, Linton MF. Leukocyte low density lipoprotein receptor (LDL-R) does not contribute to LDL clearance in vivo: bone marrow transplantation studies in the mouse. *J Lipid Res* 1997;38:391–400.
- [19] Linton MF, Hasty AH, Babaev VR, Fazio S. Hepatic apoE expression is required for remnant lipoprotein clearance in the absence of the low density lipoprotein receptor. *J Clin Invest* 1998;101:1726–36.
- [20] Muller PY, Janovjak H, Miserez AR, Dobbie Z. Processing of gene expression data generated by quantitative real-time RT-PCR. *Bio-techniques*. 2002;32:1372–1374, 1376, 1378–1379.
- [21] Millar JS, Maugeais C, Fuki IV, Rader DJ. Normal production rate of apolipoprotein B in LDL receptor-deficient mice. *Arterioscler Thromb Vasc Biol* 2002;22:989–94.
- [22] Ishibashi S, Perrey S, Chen Z, Osuga J, Shimada M, Ohashi K, et al. Role of the low density lipoprotein (LDL) receptor pathway in the metabolism of chylomicron remnants. *J Biol Chem* 1996;271:22422–7.
- [23] Twisk J, Gillian-Daniel DL, Tebon A, Wang L, Barrett PHR, Attie AD. The role of the LDL receptor in apolipoprotein B secretion. *J Clin Invest* 2000;105:521–32.
- [24] Hornick CA, Kita T, Hamilton RL, Kane JP, Havel RJ. Secretion of lipoproteins from the liver of normal and Watanabe heritable hyperlipidemic rabbits. *Proc Natl Acad Sci U S A* 1983;80:6096–100.
- [25] Millar JS, Maugeais C, Ikewaki K, Kolansky DM, Barrett PH, Budreck EC, et al. Complete deficiency of the low-density lipoprotein receptor is associated with increased apolipoprotein B-100 production. *Arterioscler Thromb Vasc Biol* 2005;25:560–5.
- [26] Mahley RW, Ji ZS. Remnant lipoprotein metabolism: key pathways involving cell-surface heparan sulfate proteoglycans and apolipoprotein E. *J Lipid Res* 1999;40:1–16.
- [27] Yu KC, Chen W, Cooper AD. LDL receptor-related protein mediates cell-surface clustering and hepatic sequestration of chylomicron remnants in LDLR-deficient mice. *J Clin Invest* 2001;107:1387–94.
- [28] Fuki IV, Kuhn KM, Lomazov IR, Rothman VL, Tuszynski GP, Iozzo RV, et al. The syndecan family of proteoglycans. Novel receptors mediating internalization of atherogenic lipoproteins in vitro. *J Clin Invest* 1997;100:1611–22.
- [29] Fuki IV, Iozzo RV, Williams KJ. Perlecan heparan sulfate proteoglycan: a novel receptor that mediates a distinct pathway for ligand catabolism. *J Biol Chem* 2000;275:25742–50.
- [30] Ebara T, Conde K, Kako Y, Liu Y, Xu Y, Ramakrishnan R, et al. Delayed catabolism of apoB-48 lipoproteins due to decreased heparan sulfate proteoglycan production in diabetic mice. *J Clin Invest* 2000;105:1807–18.
- [31] Kjellen L, Bielefeld D, Hook M. Reduced sulfation of liver heparan sulfate in experimentally diabetic rats. *Diabetes* 1983;32:337–42.
- [32] Windler E, Chao Y, Havel RJ. Determinants of hepatic uptake of triglyceride-rich lipoproteins and their remnants in the rat. *J Biol Chem* 1980;255:5475–80.
- [33] Windler E, Chao Y, Havel RJ. Regulation of the hepatic uptake of triglyceride-rich lipoproteins in the rat. Opposing effects of homologous apolipoprotein E and individual C apoproteins. *J Biol Chem* 1980;255:8303–7.
- [34] Shelburne F, Hanks J, Meyers W, Quarfordt S. Effect of apoproteins on hepatic uptake of triglyceride emulsions in the rat. *J Clin Invest* 1980;65:652–8.
- [35] Quarfordt SH, Michalopoulos G, Schirmer B. The effect of human C apolipoproteins on the in vitro hepatic metabolism of triglyceride emulsions in the rat. *J Biol Chem* 1982;257:14642–7.
- [36] Jong MC, Hofker MH, Havekes LM. Role of ApoCs in lipoprotein metabolism: functional differences between ApoC1, ApoC2, and ApoC3. *Arterioscler Thromb Vasc Biol* 1999;19:472–84.
- [37] Breckenridge WC, Little JA, Steiner G, Chow A, Poapst M. Hypertriglyceridemia associated with deficiency of apolipoprotein C-II. *N Engl J Med* 1978;298:1265–73.
- [38] Cox DW, Breckenridge WC, Little JA. Inheritance of apolipoprotein C-II deficiency with hypertriglyceridemia and pancreatitis. *N Engl J Med* 1978;299:1421–4.
- [39] Fojo SS, Brewer HB. Hypertriglyceridaemia due to genetic defects in lipoprotein lipase and apolipoprotein C-II. *J Intern Med* 1992;231:669–77.
- [40] Hegele RA, Breckenridge WC, Cox DW, Maguire GF, Little JA, Connelly PW. Interaction between variant apolipoproteins C-II and E that affects plasma lipoprotein concentrations. *Arterioscler Thromb* 1991;11:1303–9.